

USE OF SILICON SURFACE-BARRIER DETECTORS  
FOR NEUTRON DETECTION

by

G. Thomas Fairburn

Thesis submitted to the Graduate Faculty of the  
Virginia Polytechnic Institute  
in candidacy for the degree of

MASTER OF SCIENCE

in

NUCLEAR SCIENCE AND ENGINEERING

December, 1961

Blacksburg, Virginia

## II. TABLE OF CONTENTS

CHAPTER	PAGE
I. TITLE . . . . .	1
II. TABLE OF CONTENTS . . . . .	2
III. LIST OF FIGURES . . . . .	3
IV. INTRODUCTION . . . . .	5
V. REVIEW OF LITERATURE . . . . .	8
VI. APPARATUS . . . . .	12
Silicon Surface-Barrier Detectors . . . . .	12
Charge Sensitive Preamplifiers . . . . .	16
Detector Bias Supply . . . . .	22
Preamplifier Bias Supply . . . . .	23
Mercury Relay Pulser . . . . .	23
Proton Recoil Telescopes . . . . .	26
VII. PERFORMANCE AND CHARACTERISTICS . . . . .	31
VIII. INTERPRETATION OF EXPERIMENTAL DATA . . . . .	45
IX. SUMMARY . . . . .	48
X. ACKNOWLEDGMENTS . . . . .	50
XI. BIBLIOGRAPHY . . . . .	51
XII. VITA . . . . .	54

III. LIST OF FIGURES

FIGURE	PAGE
1. (a) Cross Section View of Detector, (b) Excitation of Electrons, and (c) Residual Hole-Electron Excitation . . . . .	15
2. Depletion Depth as a Function of Bias . . . . .	17
3. Schematic of RCA 7586 Nuvistor Triode Preamplifier . .	20
4. Schematic of Transistor Preamplifier Using Philco 2N393's . . . . .	21
5. Schematic of Detector Bias Supply . . . . .	24
6. Schematic of Preamplifier Bias Supply . . . . .	25
7. Schematic of Mercury Relay Pulser . . . . .	27
8. Cross Section Views of (a) Features of a Recoil Telescope, (b) Single Hole Proton Recoil Telescope, and (c) Multihole Proton Recoil Telescope . . . . .	29
9. Block Diagram of Electronics . . . . .	32
10. Pulse-Height Spectrum of Pulser Obtained With the Nuvistor Preamplifier . . . . .	33
11. Pulse-Height Spectrum of Pulser Obtained With the Transistor Preamplifier . . . . .	34
12. Pulse-Height Spectrum of $Po^{210}$ Alphas Obtained With the Nuvistor Preamplifier . . . . .	36
13. Pulse-Height Spectrum of $Po^{210}$ Alphas Obtained With the Transistor Preamplifier . . . . .	37
14. Pulse-Height Spectrum of Neutrons Obtained With the Proton Recoil Telescope . . . . .	39
15. Pulse-Height Spectrum of Neutrons Obtained With the Proton Recoil Telescope . . . . .	40

FIGURE	PAGE
16. Resultant Curves for Traverse of Thermal Column With Muistor Preamplifier . . . . .	42
17. Resultant Curves for Traverse of Thermal Column With Transistor Preamplifier . . . . .	43
18. Pulse-Height Spectrum of Modern Physics Laboratory Alpha Source . . . . .	44

#### IV. INTRODUCTION

In recent years with the development of experimental nuclear physics a need for better methods of particle detection has arisen. In response to this need came the development of the surface-barrier detectors by Mayer and Gossick (24). These surface-barrier detectors behave in many respects as thin solid-state ionization chambers (32). However, they have the advantages of being smaller and less troublesome. These detectors are now being employed in the detection of charged particles, such as fission fragments, alpha particles, and protons. Beta particles of sufficiently low energy may also be detected. Neutrons may be detected if some intermediary reaction is employed which has a charged particle as a reaction product. It is this last purpose that is being given the greatest consideration in this research.

At present there are two important methods of neutron detection using the surface-barrier detectors. In general, neutrons are detected by the reaction of the neutron with a radiator material, such as  $\text{Li}^6$  or  $\text{B}^{10}$ , producing one or more charged particles. A neutron detector using  $\text{Li}^6$ , for example, usually consists of a thin layer of  $\text{Li}^6$  deposited between two silicon surface-barrier detectors (20). The neutrons are detected by observing the  $\alpha$  and T pair resulting from the  $\text{Li}^6(n, \alpha)\text{T}$  reaction. With this sandwich geometry the energy of the neutron can be determined from the sum of the pulses in the two detectors arising from the simultaneous detection

of both reaction products. Boron-10 may be used in a similar fashion by depositing a thin layer on or near the sensitive area of the detector (23). In this method a slow neutron is captured and the alpha particle resulting from the  $B^{10}(n, \alpha)Li^7$  reaction is detected. However, in this type of detector the energy of the incoming neutron is not as easily determined and it is generally used only for the detection of thermal neutrons.

The second method consists of the detection of recoil protons which occur when a hydrogenous material is bombarded by fast neutrons (10, 15, 38). The energy of the incoming neutron can be directly determined by measuring the energy of the recoil proton (1, 11, 31). Since the scattering of fast neutrons by protons is elastic and isotropic in the center-of-mass system up to quite high energies, it is possible to specify the energy of a neutron incident from a given direction in terms of the energy and direction of the recoil proton (7). This then leads to the possible development of a neutron spectrometer which could operate over a wide energy range and could give valuable information about the distribution of neutron energies, for example, in a reactor.

In either of the above methods of neutron detection special equipment is required, some of which was not available as stock items. The construction of this equipment constituted the preliminary phase of the experiment.

The second phase of the experiment was the employment of this equipment and the silicon surface-barrier detectors for neutron detection. This research also has the ultimate aim of leading to the production of a neutron spectrometer for application with the V.P.I. reactor.

## V. REVIEW OF LITERATURE

The recent interest in the use of semiconductor devices as particle detectors is an outgrowth of earlier work on crystal counters. The principle of operation of the crystal counter is similar to the present junction detectors. A particle incident on the crystal has an ionizing action producing hole-electron pairs in the interior of the crystal across which an electric field has been established. The holes and electrons drift under the action of the applied field. As the carriers move they induce charge on the plates proportional to the potential difference they traverse.

Thus in order to utilize the high fields and low leakage currents of semiconductor devices, McKay (25) used point contact rectifiers and p-n junctions as charged particle detectors. In the case of the p-n junctions the particles were incident parallel to the junction. With this geometry, particles striking the device away from the junction create carriers which tend to recombine before diffusing to the junction. The response of the diode is thus a function of the distance from the junction at which the carriers are created.

Shortly after the successful investigation on p-n junctions by McKay, the use of semiconductor devices as alpha particle spectrometers was demonstrated by Mayer and Gossick (24). The



geometry of their device allowed the particle to be incident normal to the plane of the junction. This geometry resulted in a uniform response to charged particles with very good resolution.

Since early 1959, intensive programs have been initiated at several laboratories to determine the capability of silicon junctions to perform as charged particle spectrometers. The choice of silicon was determined by its low junction leakage current under reverse bias. Most of the initial work was performed at Oak Ridge National Laboratory by Walter et al. (35,36,37). From the extensive measurements performed by them on semiconductor surface-barrier detectors, it was concluded that the detectors were excellent for short-range particle detection. Other conclusions were that the detectors exhibited good resolution and pulse-height linearity if the range of the particle does not exceed the detector depletion depth. These detectors have other features aside from linearity and good resolution. They are compact in size with a sensitive area usually less than 1 square centimeter, although they are available with areas as large as 3.8 square centimeters. The absence of a physical window over the sensitive area allows low energy particles to enter. Two of their most important advantages are their relative insensitivities to background radiation, such as gamma rays, neutrons, and fast charged particles, and to effects of magnetic fields. An additional advantage is the ability to change the sensitive region simply by varying an external bias voltage.

Blankenship and Bowkowski (3,4), Halbert and Blankenship (13), and Halbert, Blankenship, and Goldman (14) have used thin monoenergetic alpha sources to determine the resolution of silicon surface-barrier detectors.

Since these detectors are sensitive to charged particles, the use of proton recoil telescopes as a means of neutron detection is feasible. Most of the previous recoil proton research was performed using proportional counters as detectors. Cochran and Henry (7), Johnson and Trail (17), and Perlow (30) have reported results for the resolution obtained in this manner. In section VIII the results obtained by the author using silicon surface-barrier detectors are compared with their results. The small silicon surface-barrier detectors can be applied to any charged particle problem where good resolution is required, but the counting rate may be poor, since the net efficiency is generally low.

With the development of the surface-barrier detector came the need for better electronics (2,4,6,18). The first change that occurred was the development of the charge sensitive preamplifier since the signal coming from the detector should be proportional to a charge instead of a voltage. Another change was the development of fast electronics. There are certain advantages that are obtained by making the preamplifier fast. A noise signal arises from the device leakage current. Generally this current exhibits a  $f^{-\alpha}$  dependence on frequency, where  $\alpha$  is close to unity. Also the total grid circuit

impedance behaves like  $f^{-1}$ , since it is essentially a capacitance. Thus it follows that the noise voltage varies as  $1/f$  to some power. However, the detector signals are fast, and hence, if fast electronics are employed it is possible to use a short clipping time and be well removed from the high noise region.

Research is still progressing to improve these detectors. Bigger depletion depths are being obtained by diffusing lithium ions into heated high resistivity silicon. Silicon is being purified more to obtain higher resistivities. Larger surface areas are being used to increase the efficiency of the detectors since the efficiency is fairly low in the present detectors. Better resolution detectors are also being developed. With the expected progress in all these areas a very competitive detector should be produced in the near future.

## VI. APPARATUS

### Silicon Surface-Barrier Detectors

The manufacturing of surface-barrier detectors is basically simple. Single-crystal material is cut into 1 mm-thick wafers of the desired sensitive area. The wafers are carefully lapped and a copper wire or foil is soldered to one face to make an ohmic contact with the body of the crystal. With a germanium crystal, one can solder directly to the surface, however, with silicon the surface is first nickel plated. The crystal is then cast in some material, such as an epoxy resin, so that the opposite face is exposed. The exposed surface is then etched in a solution of nitric, hydrofluoric and glacial acetic acids. One creates a rectifying junction in the crystal, i.e. in silicon, in one of two ways. In the first method a donor material (phosphorous is most commonly used) is diffused into p-type silicon so as to create an n-type region at the surface of the silicon wafer. In the second method the surface of n-type silicon is coated with gold by evaporation to produce an extremely thin p-type inversion layer. A lead is then attached to the surface adjacent to the junction material. This lead and the ohmic contact thus produce a diode.

Extreme care must be taken in all steps and processes of manufacturing in order to achieve a high proportion of successful detectors. If the surface has been carefully prepared so it is

free of irregularities which would degrade the resolution, the major problem is to keep the noise level as low as possible. The detector noise can be greatly attenuated by the selection of highly perfect crystals, meticulous cleanliness, and thorough rinsing after etching.

A cross sectional view of the gold-n-type silicon detector of the type employed in this research is given in figure 1(a). The sensitive area H is a square and can be seen as a raised flat portion of the surface. Lead C is the signal output and bias voltage connection. Lead J is a thin pretinned copper strip for a soldered ground connection. I is the epoxy resin which separates pin C electrically from the thin gold layer on the crystal surface. The epoxy resin also serves as a rugged mounting for the silicon wafer S.

The theory behind the operation of these detectors is essentially derived from solid state physics. Energetic particles lose energy rapidly through interaction with electrons in solids. In a semiconductor these collision processes may lift electrons from the valence band to the conduction band, but they may also lift electrons from the deeper lying occupied bands to bands that are higher than the conduction band. This is shown in figure 1(b). These electrons now appear in normally unoccupied bands creating holes in the normally full bands. This condition persists for only about  $10^{-12}$  seconds. The interactions among the electrons make the electrons fall to the bottom of the lowest lying level in the conduction band and the interactions among the holes make the holes

rise to the top of the valence band. This is shown in figure 1(c). Furthermore, during this energetic Auger de-excitation process, many more holes and electrons are created. On the average the many-step process results in the creation of one hole-electron pair for each  $3.6 \pm 0.3$  ev of energy lost by the incident heavy particle (26). This is about three times the energy gap,  $E_g$ , for silicon. The final step in the de-excitation is the recombination of the electrons and holes.

The range of the low energy knock-on electrons is short in solids. Consequently the path of the primary heavy particle is marked by a rather thin, cylindrically shaped plasma of holes and electrons.

If a reverse biasing voltage is applied to the detector an electric field will be established at the junction and a small leakage current, of the order of a fraction of one microampere, will flow across it. Within the silicon essentially all of the reverse biasing voltage appears across the so-called depletion layer. The depletion layer is the sensitive region of the device, and if charge carriers are generated within it by the passage of a nuclear particle they will be swept apart just as they are in a gas-filled ion chamber.

A significant difference between a solid state detector and an ionization chamber is that the density of the medium is much greater than that of the gas in the ion chamber, thus the ranges of heavy particles are measured in microns rather than centimeters.

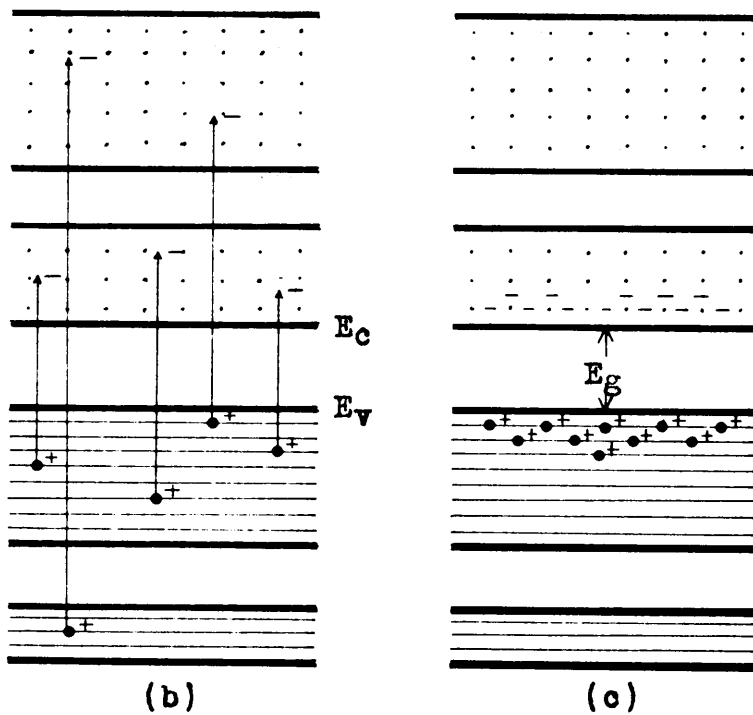
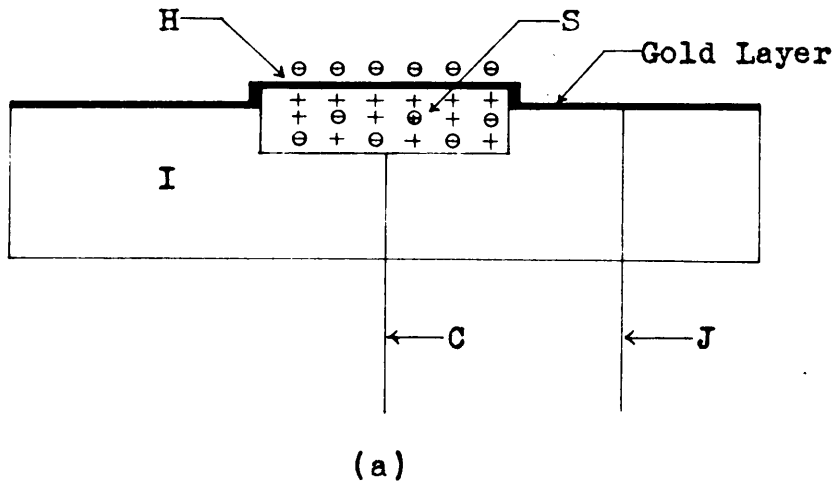


Figure 1. (a) Cross section view of detector, (b) excitation of electrons, and (c) residual hole-electron excitation.

Another difference is in the nature of a complication. The width of the depletion region, corresponding to the distance between parallel plates of a simple ion chamber, varies as the square root of the applied bias voltage. Correspondingly the junction capacitance is proportional to the inverse of the square root of the bias voltage. Thus silicon surface-barrier detectors are like ion chambers whose plates move as a function of applied voltage. The depletion depth is shown as a function of the bias voltage in figure 2.

#### Charge Sensitive Preamplifiers

The signal voltage produced by a detector is a function of the applied bias since the detector capacitance is bias dependent. Furthermore, the quantity of interest is not actually the voltage but the total charge,  $Q$ . For this reason it has been found necessary to employ charge sensitive electronics. The charge released in the depletion region of the detector is proportional to the energy lost by the charged particle in passing through this region. The detector capacitance is proportional to the junction area and inversely proportional to the square root of the bias voltage. This is given by

$$C_d = A_d C_o / (e n v)^{\frac{1}{2}}$$



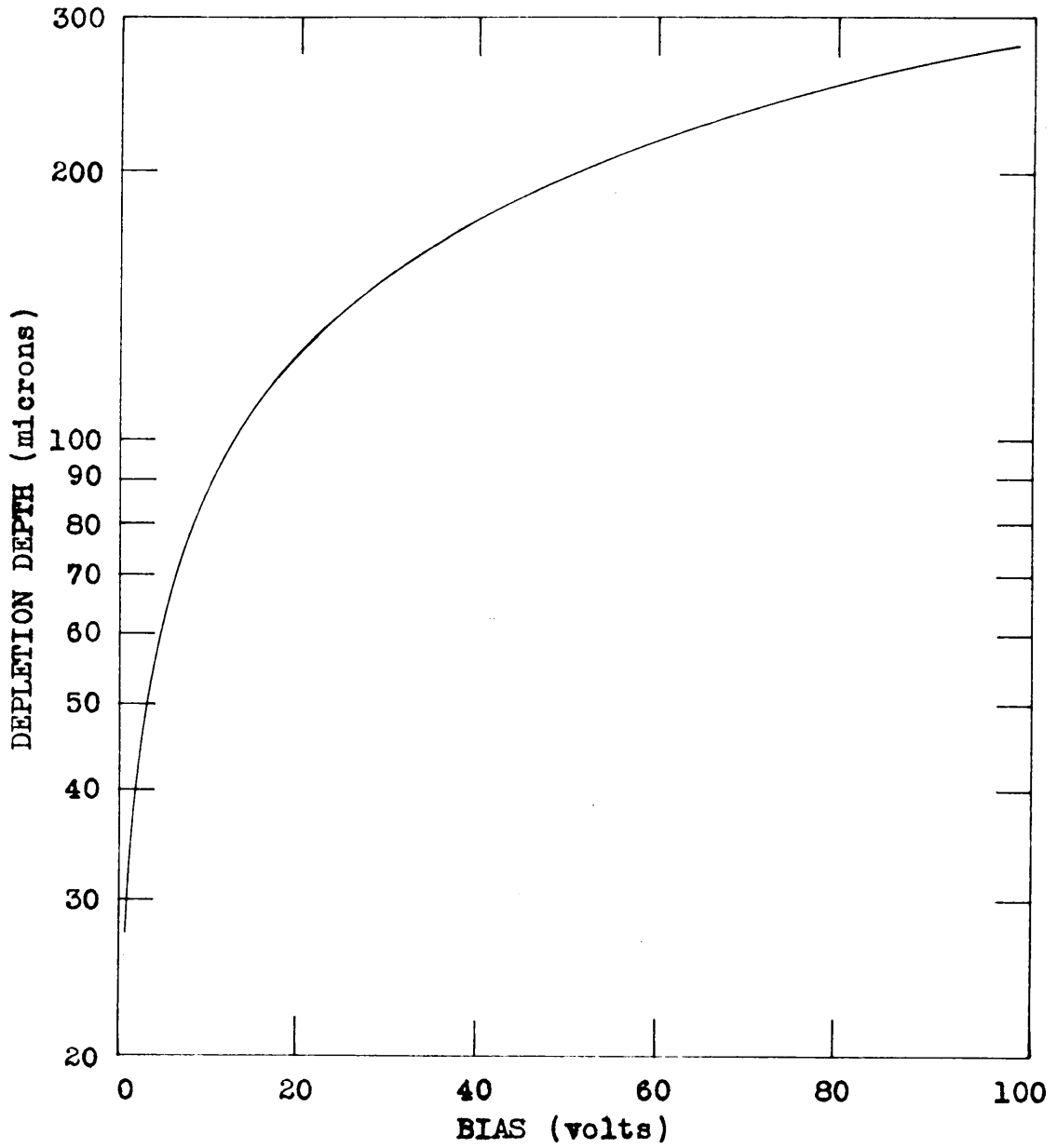


Figure 2. Depletion depth as a function of bias.

where

$$C_0 = 210\text{pf (volts)}^{\frac{1}{2}}(\text{ohm-cm})^{\frac{1}{2}}/\text{mm}^2,$$

$\rho_n$  = n-type silicon resistivity (ohm-cm),

$A_d$  = detector sensitive area ( $\text{mm}^2$ ),

and

$V$  = applied bias (volts).

This difficulty can be greatly relieved by the use of negative capacitive feedback which attenuates the influence of the detector capacitance on the signal. Negative feedback tends to maintain constant charge sensitivity for different bias voltages. Therefore, the output pulse from the preamplifier is proportional to the charge released in the detector and independent of the preamplifier input capacitance. This is given by

$$\text{OUTPUT} = Q/C_f$$

where

$Q$  = amount of charge at preamplifier input

and

$C_f$  = feedback capacitance.

The pulse height signal from the detector is given by

$$V = Q/C_{\text{total}}$$

where

$Q$  = charge produced by the incident particle

and

$$C_{\text{total}} = C_d + C_{\text{stray}}$$

Therefore, it is helpful to have the detector as close as possible to the preamplifier. In order to accomplish this, the signal inputs to the preamplifiers were built to accommodate the detector base fitting.

The nuvistor preamplifier is built in the form of a rectangle with dimensions of 1.25 x 1.25 x 22 inches. The transistor preamplifier is a cylinder with dimensions of 0.75 x 4.6 inches.

The circuit of the RCA 7586 Nuvistor triode preamplifier is shown in figure 3. Of the various low noise tubes which are suitable for the preamplifier, the 7586 was used because it is much less microphonic than the 417A, which would otherwise have been the first choice. This factor could be important when operating near an accelerator. This circuit makes use of a long-tailed-pair as the second stage to reduce the Miller effect. The first stage is a cascode stage, and the last is a cathode follower to drive the output cable. The only critical feature is the isolation of the input so that the stray capacitance does not affect the negative feedback. The circuit has a measured rise time of 1  $\mu$ sec. and a decay time of 30  $\mu$ sec. The amplification of this preamplifier is approximately 130, with a kev-equivalent noise (fwhm) of approximately 11 kev.

The circuit for the transistor preamplifier using the Philco 2N393's is given in figure 4. Transistors T<sub>1</sub> and T<sub>2</sub> form a cascode stage similar to the first stage in the circuit of figure 3. The

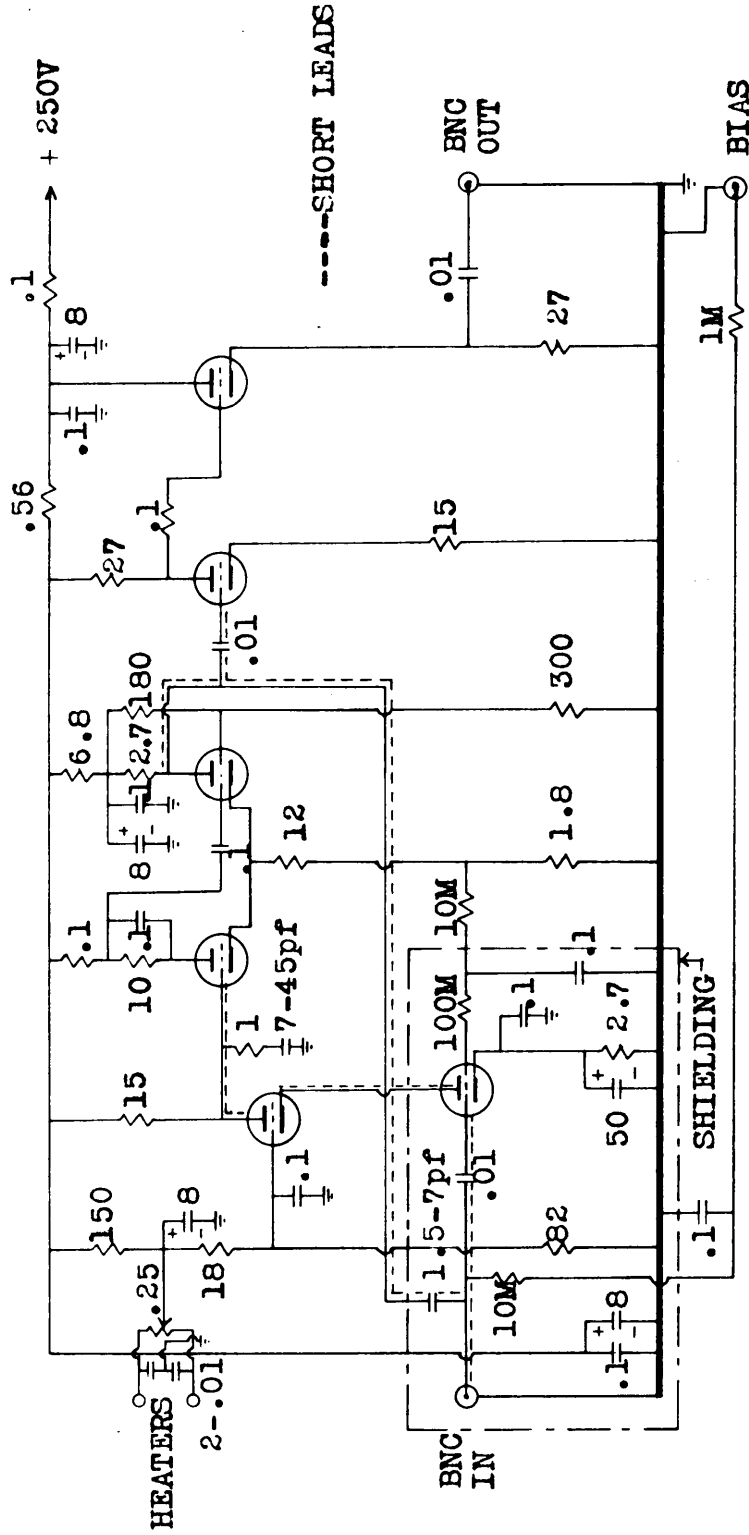


Figure 3. Schematic of RCA 7586 Nuvistor triode preamplifier. All resistors are in kilo-ohms and capacitors are in micro-farads unless otherwise indicated.

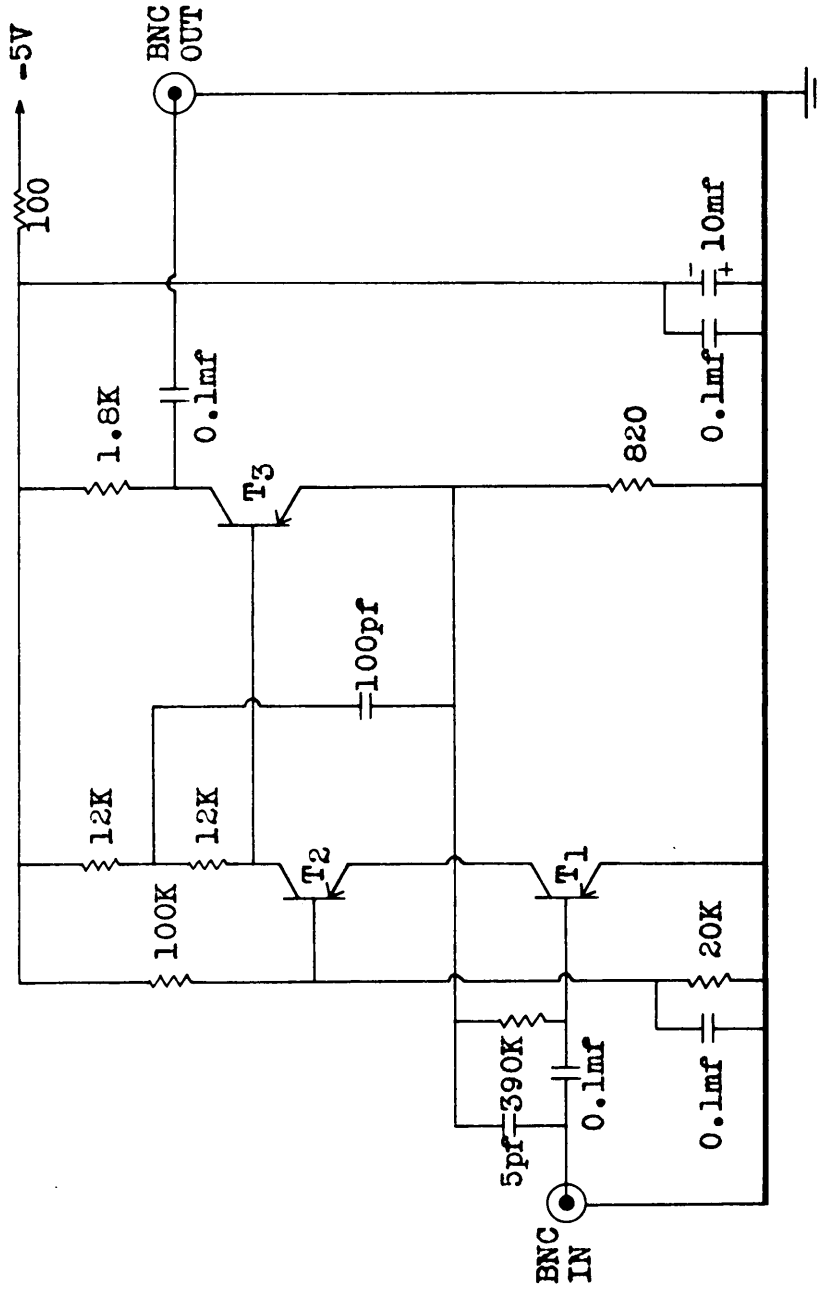


Figure 4. Schematic of transistor preamplifier using Philco 2N393's.

output of the circuit taken from the collector of  $T_3$  is similar to a cathode follower stage normally used to drive an output cable. The amplification of this preamplifier is approximately 27. The measured rise and decay times are  $0.8 \mu\text{sec.}$  and  $7 \mu\text{sec.}$  respectively. The kev-equivalent noise (fwhm) is about 13 kev.

The kev-equivalent noise (fwhm) was determined by the following formulae:

$$N(\text{fwhm}) = 5.83 \times 10^{16} E_p C_p E_{\text{rms}} / E_o$$

where

$E_p$  = output voltage at pulser,

$C_p$  = coupling capacitance in farads (lpf),

$E_{\text{rms}}$  = RMS noise voltage at amplifier with the pulser turned off,

and

$E_o$  = output voltage of preamplifier.

$E_p$  and  $E_o$  can be measured directly on an oscilloscope. However,  $E_{\text{rms}}$  was a little difficult to obtain, since a low range rms voltmeter was not available. The peak to peak voltage at the output of the preamplifier with the pulser turned off was measured on a tektronix 545 oscilloscope and then divided by one over the square root of two to obtain the approximate rms value.

#### Detector Bias Supply

The detector bias supply is a network of batteries which can supply a very stable voltage from 0-100 volts in 1.4 volt steps to the detector. The bias is applied to the detector through an RC

filter and a 10 megohm protective resistor both of which are built into the preamplifiers. Provisions have been made to read the bias voltage up to 100 volts and the detector current over a range of 0.1  $\mu$ amp to 15  $\mu$ amp. However, the normal operating current of the detector is on the order of a few tenths of a microampere. Since the operating current of the detector is quite low, the current being drained from the bias supply is low, therefore, the characteristics of the batteries are essentially those of shelf stored batteries. A schematic diagram of the bias supply is shown in figure 5.

#### Preamplifier Bias Supply

The preamplifier bias supply also uses batteries as a voltage source yielding a very stable voltage supply. The bias supply was variable in order that the voltage applied to the transistor preamplifier could be maintained at a particular value, i.e. -5.0 volts. The large load resistor limits the amount of current drained from the battery in order to prolong the life of the battery. A schematic diagram of the bias supply is shown in figure 6.

#### Mercury Relay Pulser

The mercury relay pulser provides a convenient way of testing and adjusting the electronic equipment. The relay provides 60 pulses per second which have a rise time of 0.01  $\mu$  sec and a decay time of 40  $\mu$  sec with a variable pulse height. The pulser provides

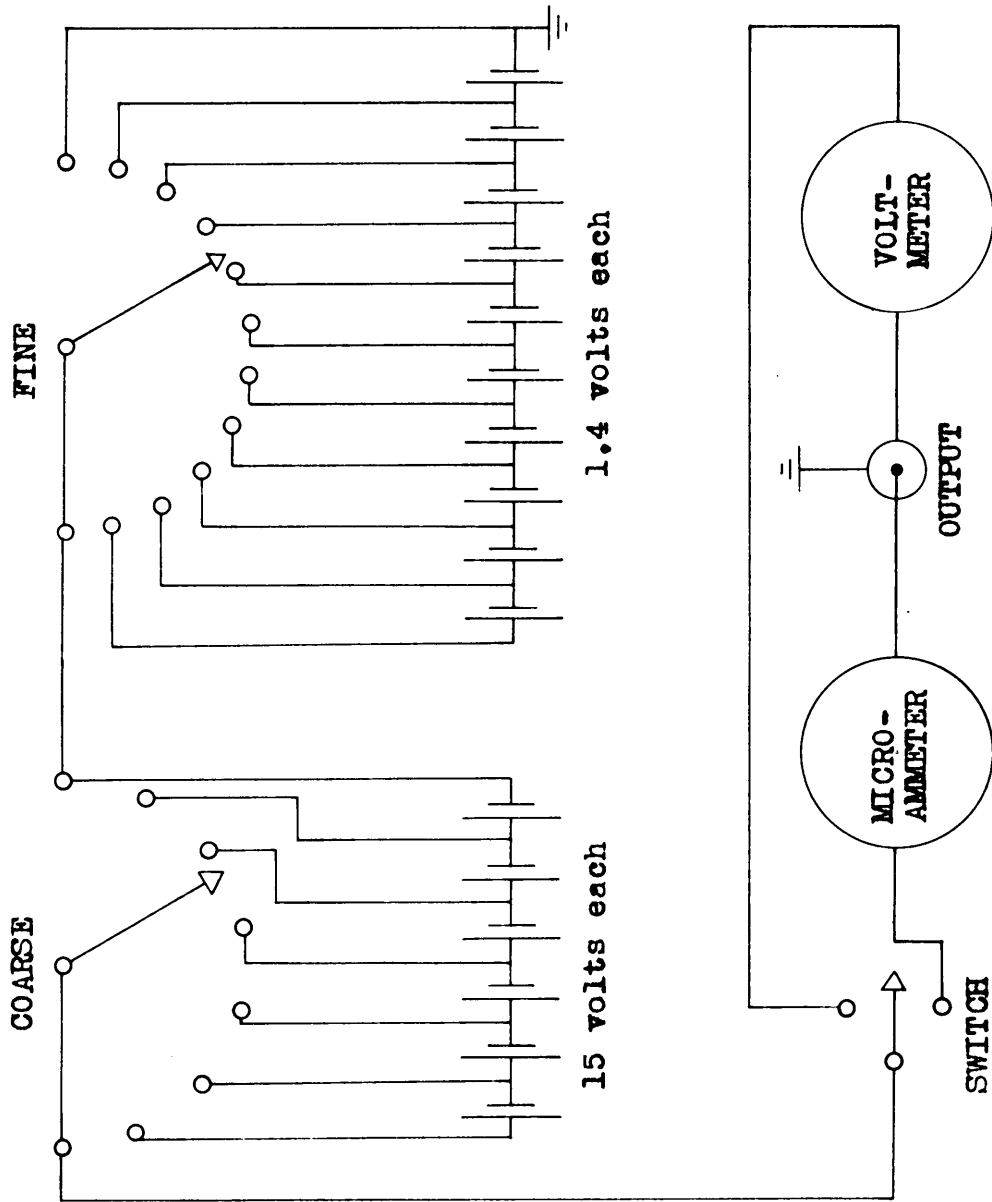


Figure 5. Schematic of detector bias supply.



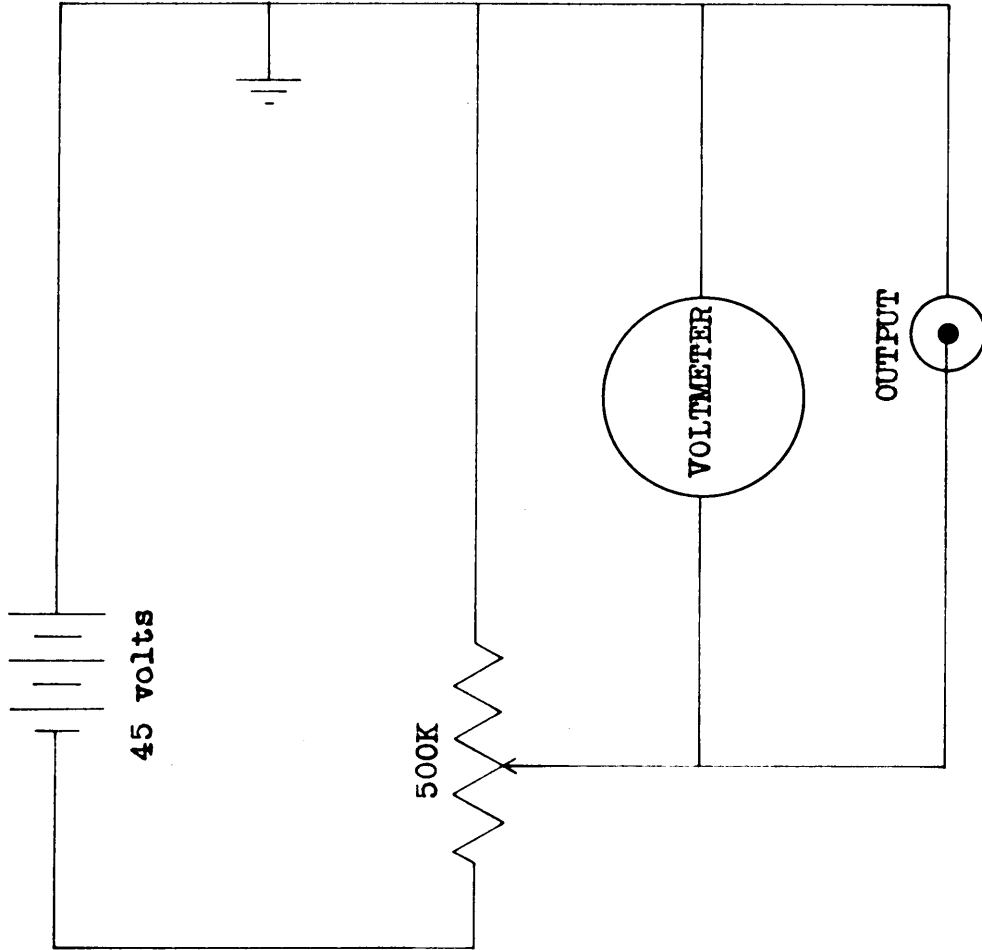


Figure 6. Schematic of preamplifier bias supply.

a standard signal which may be used to adjust the pulse shape in the preamplifier and to measure the gain of the preamplifier and the resolution of the electronic equipment. The pulser is connected to the detector input through a 1 pf capacitor, which simulates a signal from the detector. A one volt pulse through the 1 pf capacitor is approximately equivalent to a 1.78 mev particle pulse. The schematic diagram of the pulser is shown in figure 7.

#### Proton Recoil Telescope

As previously mentioned one method of determining the energy of neutrons is by measuring the energy of recoil protons from an hydrogenous radiator. In the laboratory system, let  $E_n$  be the energy of the neutron before collision and  $\theta$  the angle between the paths of the incoming neutron and the recoil nucleus. From the conservation of energy and momentum, the energy  $E$  of the recoil nucleus is

$$E = \frac{4A}{(1+A)^2} E_n \cos^2 \theta$$

where  $A$  is the mass number of the recoil nucleus. The recoil energy is a maximum for a "head-on" collision ( $\theta = 0$ ), in which case the energy  $E_{\max}$  of the recoil nucleus is

$$E_{\max} = \frac{4A}{(1+A)^2} E_n .$$

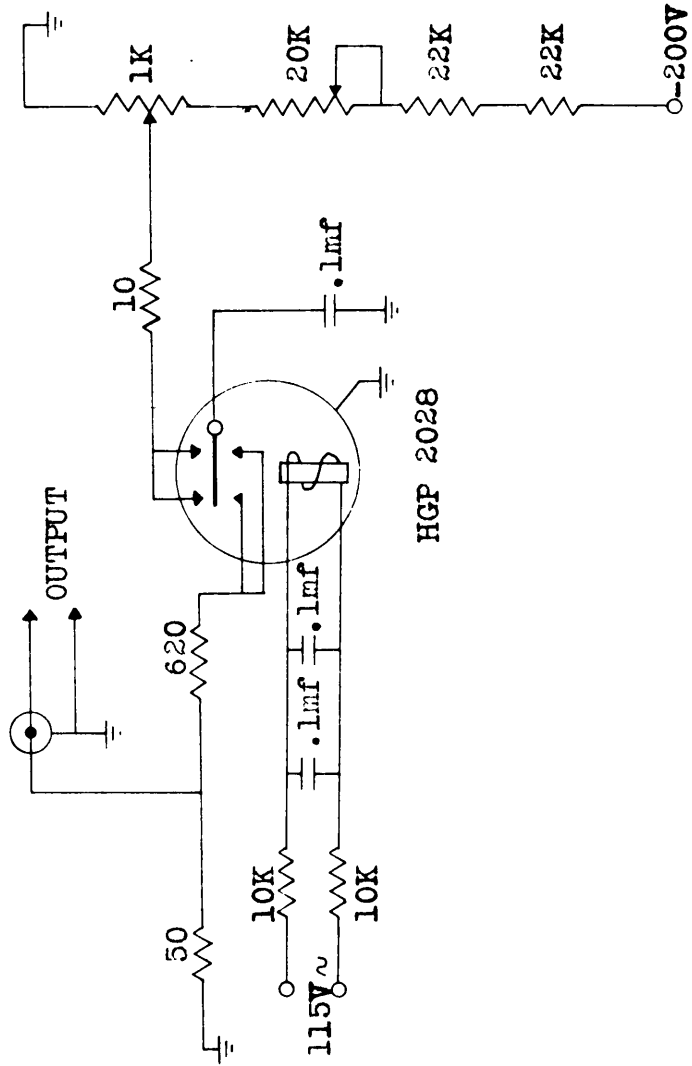


Figure 7. Schematic of mercury relay pulser.

Hydrogen is an excellent radiator for recoil telescopes for several reasons. At most energies its scattering cross section is appreciably larger than most other light nuclei. The cross section is a smooth function of energy, and the energy of the recoil hydrogen atom is larger than that of any other nuclide.

For hydrogen, which has an A of one, the energy  $E_p$  is

$$E_p = E_n \cos^2 \theta$$

With a maximum energy

$$E_{\max} = E_n.$$

With the foregoing theory in mind a proton recoil telescope can now be constructed. In terms of resolution, the thickness of the radiator material and the geometric acceptance angle are the two most critical parameters. A diagram of the general features of a recoil telescope is shown in figure 8(a). The incoming neutron  $n$  strikes the radiator material  $R$  and knocks a proton out of the material. The recoiling proton  $p$  will pass through the detector aperture  $C$  if the angle  $\theta$ , which is the angle between the paths of the two particles, is less than the maximum angle  $\theta_{\max}$ , determined by the geometry of the telescope. After passing through the aperture the proton strikes the sensitive area of the detector and is detected when it loses its energy in the depletion layer of the detector. In this experiment 0.00025 inch mylar, a hydrogenous material, was used as the radiator and the detector apertures were defined by aluminum

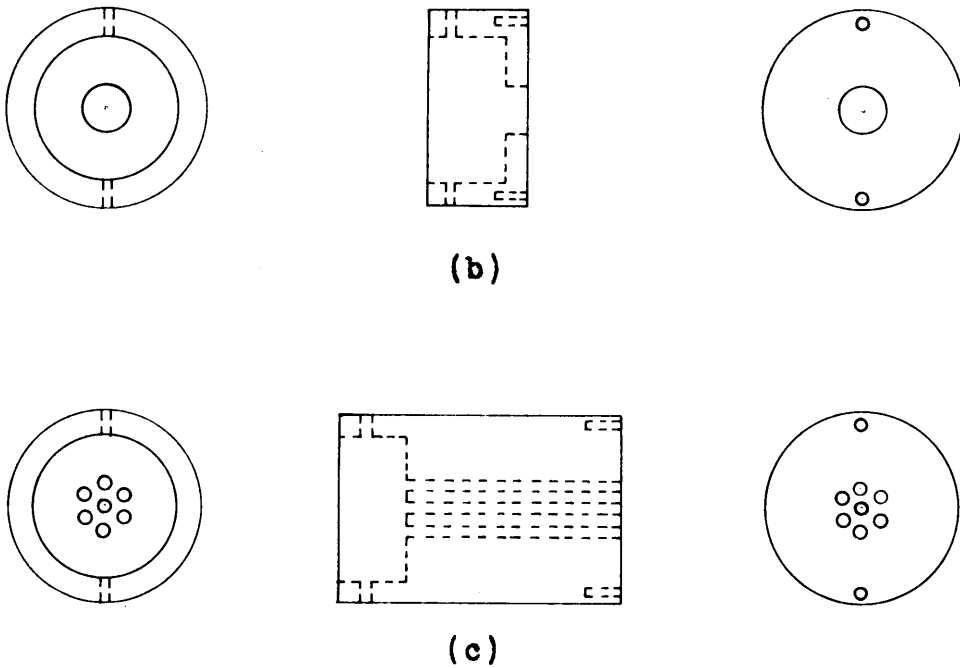
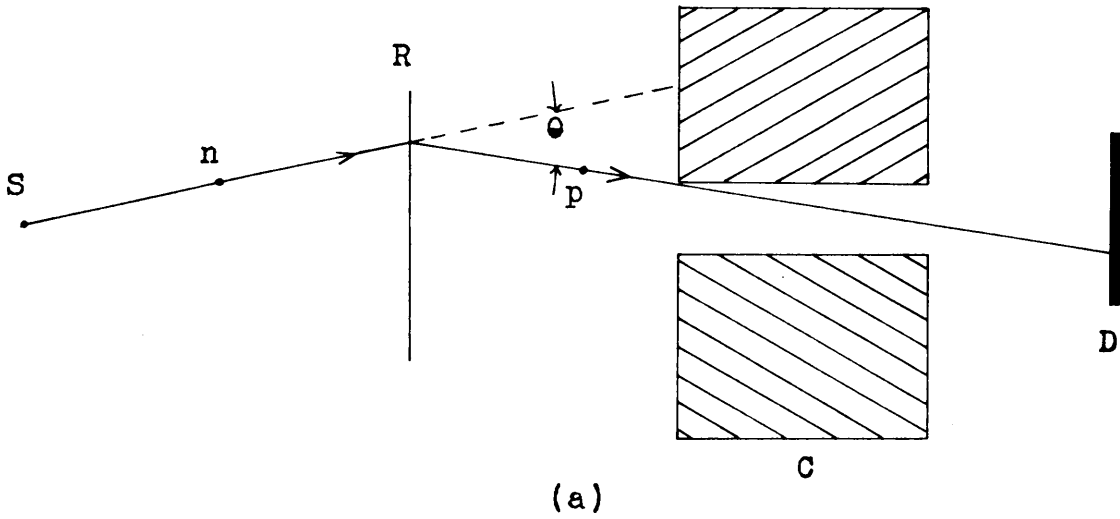


Figure 8. Cross section views of (a) features of a recoil telescope, (b) single hole proton recoil telescope, and (c) multihole proton recoil telescope.

collimators. Cross sectional views of the two geometries that were tried are shown in figure 8(b) and (c). The actual data shown later in section VII were taken using the telescope with the single aperture. This telescope was used in preference to the multihole one since resolution could be sacrificed in order to obtain a higher counting rate. Resolution was not the primary interest at this stage in the development of a neutron spectrometer based on the detection of recoil protons, but rather to show the feasibility of such an instrument.

The geometrical resolution of this telescope was calculated to be 5.4 per cent. Protons recoiling at a small angle  $\theta$  have energy  $(1-\theta^2)E_n$ , so that the resolution width resulting from the angular acceptance is a function of some average angle,  $\theta_0$ . A numerical integration over the areas of the radiator and detector shows that  $\theta_0$  refers to protons passing from the edge of the radiator to the center of the detector, if the detector and aperture are the same size. The average angle  $\theta_0$  and hence the geometrical resolution were calculated from the physical dimensions of the telescope. In this case the detector is slightly smaller, but this would only make the calculated geometrical resolution larger than it actually was.

## VII. PERFORMANCE AND CHARACTERISTICS

The block diagram of the equipment employed in performing this experiment is shown in figure 9. The amplifier is a linear amplifier, Model 218, manufactured by Baird-Atomic. The pulse analyzer is the 512 channel Nuclear Data Model 120. The other components are the equipment constructed for use with the silicon surface-barrier detectors and described in the previous section.

There are two basic methods for checking the characteristics of the detector and associated electronic equipment. A pulse from the pulser may be fed through the 1 pf capacitor into the entire system and a pulse-height spectrum taken. The results of this test are shown in figures 10 and 11 for the muvistor and transistor preamplifiers respectively. The full width at half maximum was measured and from this the resolution was calculated from the ratio of the width at half maximum to the peak position. For the muvistor preamplifier the resolution was 0.59 per cent and for the transistor preamplifier it was 0.48 per cent.

The second method of checking the system characteristics employs a monoenergetic alpha source and includes the effects of the surface-barrier detector. The source used was  $\text{Po}^{210}$  which emits only a 5.3 mev alpha particle. In this method the alpha particles are detected by the silicon detector and the resulting pulses amplified by the electronics. A pulse-height analysis as in the

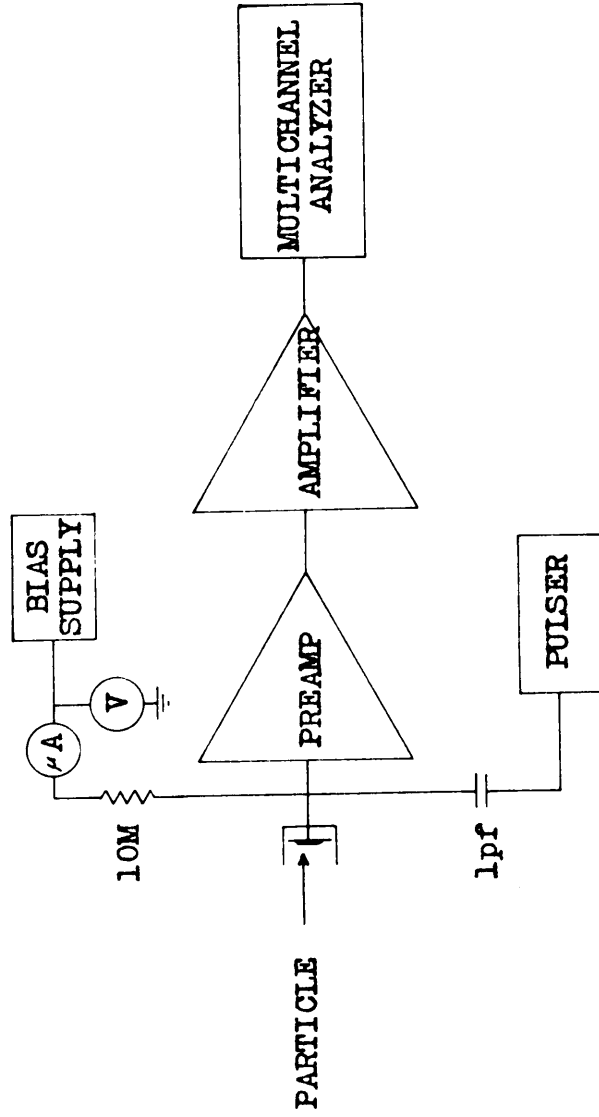


Figure 9. Block diagram of electronics.



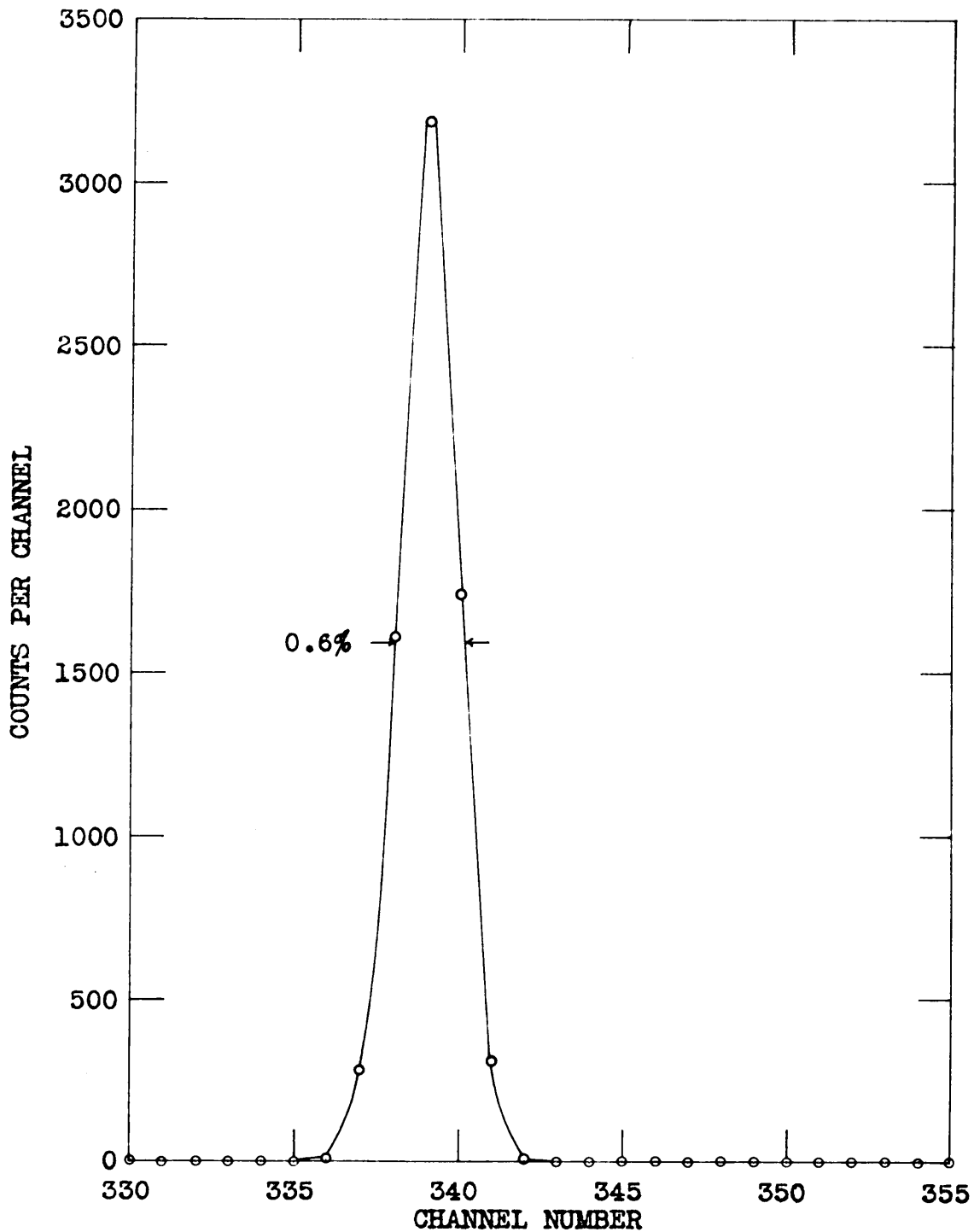


Figure 10. Pulse-height spectrum of pulser obtained with the nuvistor preamplifier.

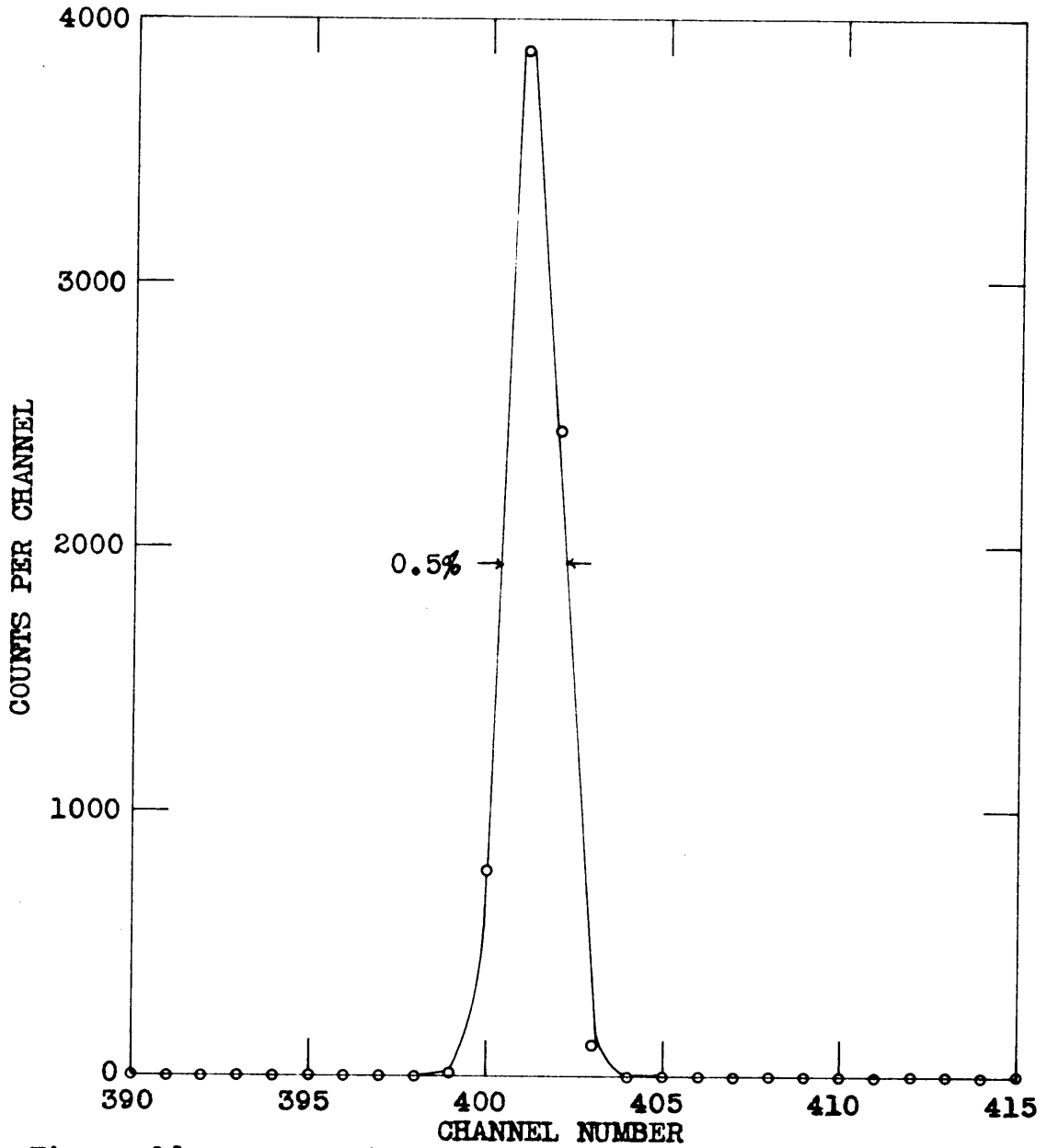


Figure 11. Pulse-height spectrum of pulser obtained with the transistor preamplifier.

previous method yields the resolution of the entire system. The results of this test are shown in figures 12 and 13 for the muvistor and transistor preamplifiers respectively. The resolution obtained for the muvistor preamplifier was 3.8 per cent and for the transistor version it was 7.0 per cent. There is a considerable difference in the results obtained for the two preamplifiers. This difference may probably be attributed to the source. The muvistor preamplifier was constructed first and thus was tested when the alpha source was new. The transistor preamplifier was constructed much later. In the meantime the alpha source had been used many times and the surface very likely could have been contaminated. Even a moderately thin amount of dust or grease upon the surface would cause straggling and hence poor apparent resolution.

After performing these checks on the characteristics of the detector and associated electronic equipment, a recoil proton telescope was constructed to test the feasibility of this approach to the problem of constructing a neutron spectrometer. The d-d reaction from the Cockcroft-Walton accelerator was used for the neutron source as it was the most monoenergetic neutron source available. The detector was set up at a back angle of approximately  $176^\circ$ . At this angle the energy of the produced neutrons varies very little as a function of deuteron energy. Hence the straggling of the deuteron in the thick drive-in target and variations of the deuteron energy would not be important. The energy of the neutrons

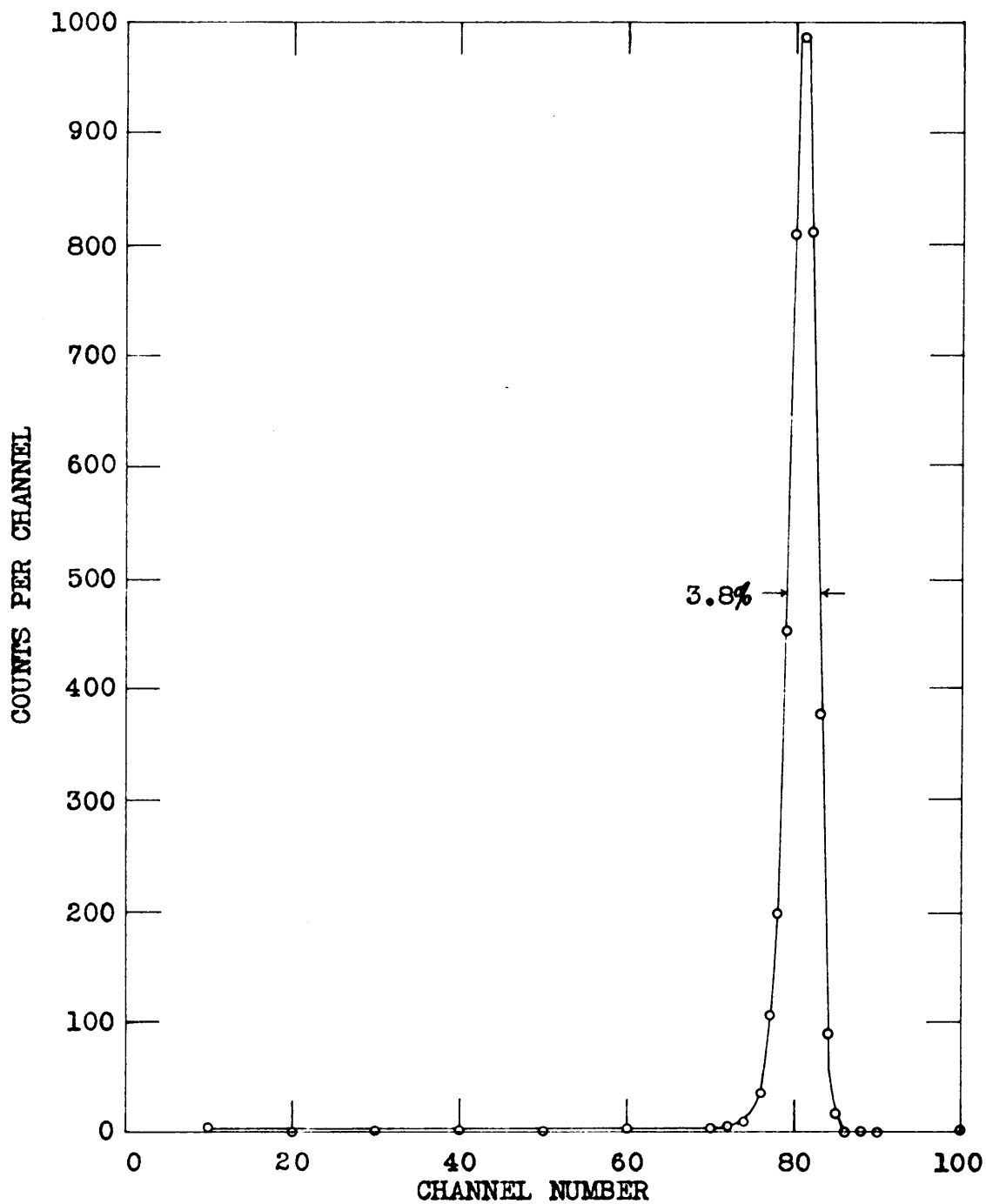


Figure 12. Pulse-height spectrum of  $Po^{210}$  alphas obtained with the nuvistor preamplifier.

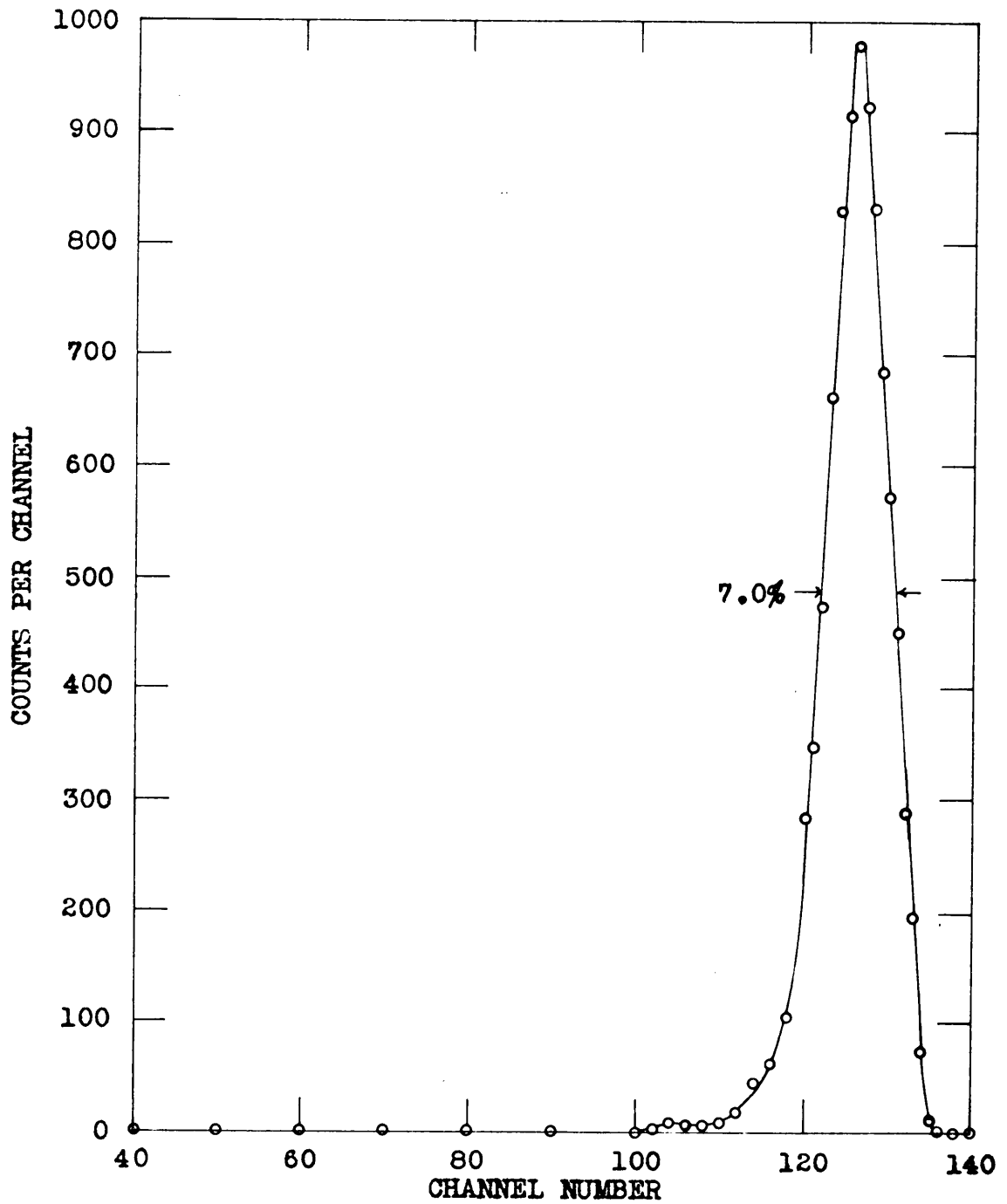


Figure 13. Pulse-height spectrum of  $Po^{210}$  alphas with the transistor preamplifier.

produced by the Cockcroft-Walton were approximately 2.1 mev. The bias on the detector was set at 26 volts in order to have a depletion layer deep enough for protons of this energy to deposit all their energy. The response of the telescope to these neutrons for the original and confirming run are shown in figures 14 and 15 respectively. The resolutions obtained were 8.4 per cent and 7.3 per cent respectively. All of this resolution can be accounted for from the design parameters of the telescope. As stated previously the geometrical resolution of the telescope was 5.4 per cent. The energy spread of the recoil proton contributed by the radiator itself is the largest source of error. The chemical name of mylar is polyethylene terephthalate. Exact information on the energy loss for a proton passing through mylar was not available, however, tables of energy losses in similar organic compounds are available (23) so an estimate of 7 per cent for the energy spread from the radiator was made by comparison with these tables. The total resolution then is given by taking the square root of the sum of the squares of each individual energy spread. From this the theoretical resolution for the spectrum was 8.9 per cent. This is higher than the experimental resolution since the largest possible assumptions were made in calculating the theoretical resolution.

An additional experiment was performed using the detector as a thermal neutron detector. The radiator for this experiment was constructed of a thin polystyrene cap with a small deposit of  $B^{10}$

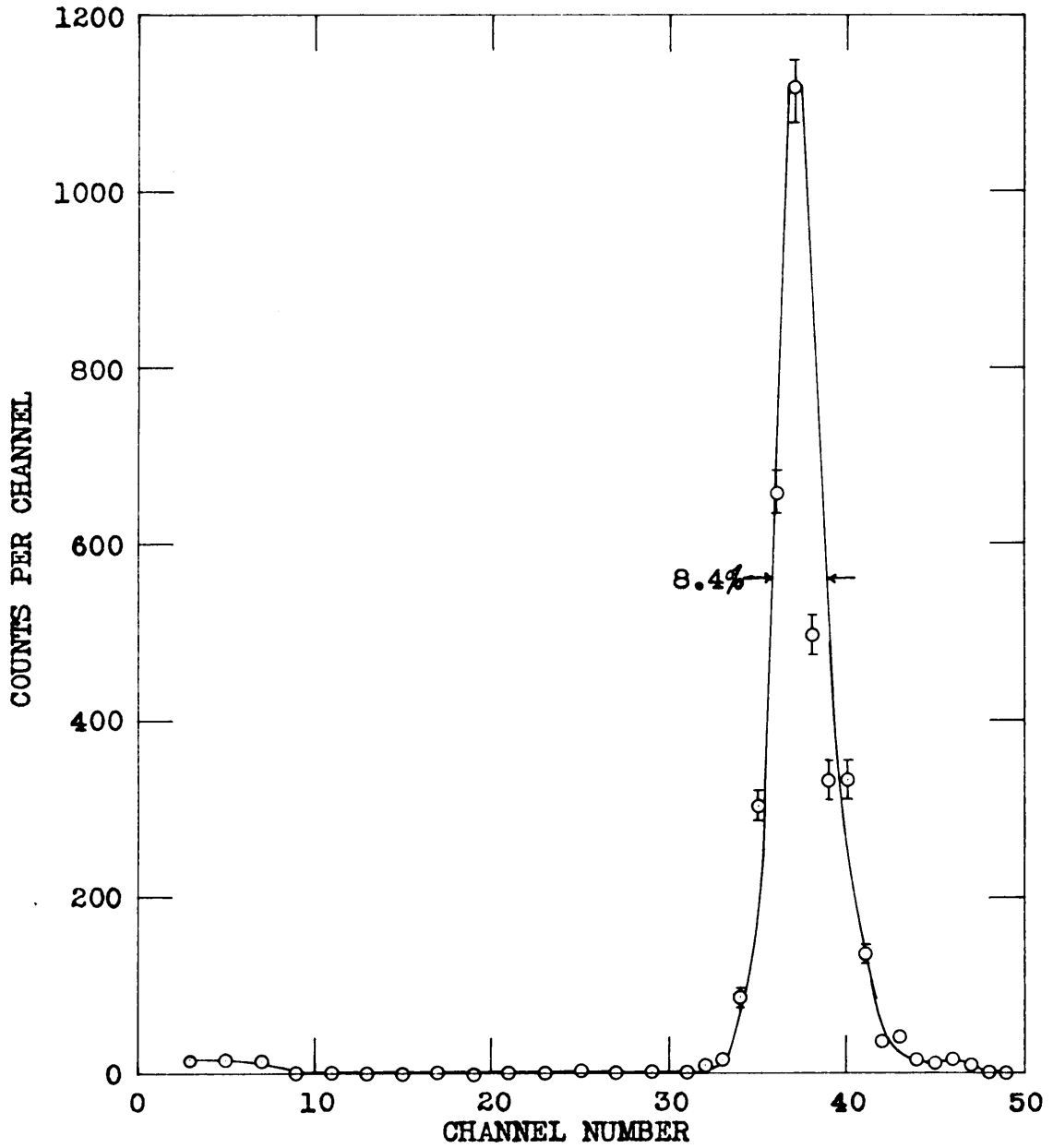


Figure 14. Pulse-height spectrum of neutrons obtained with the proton recoil telescope.

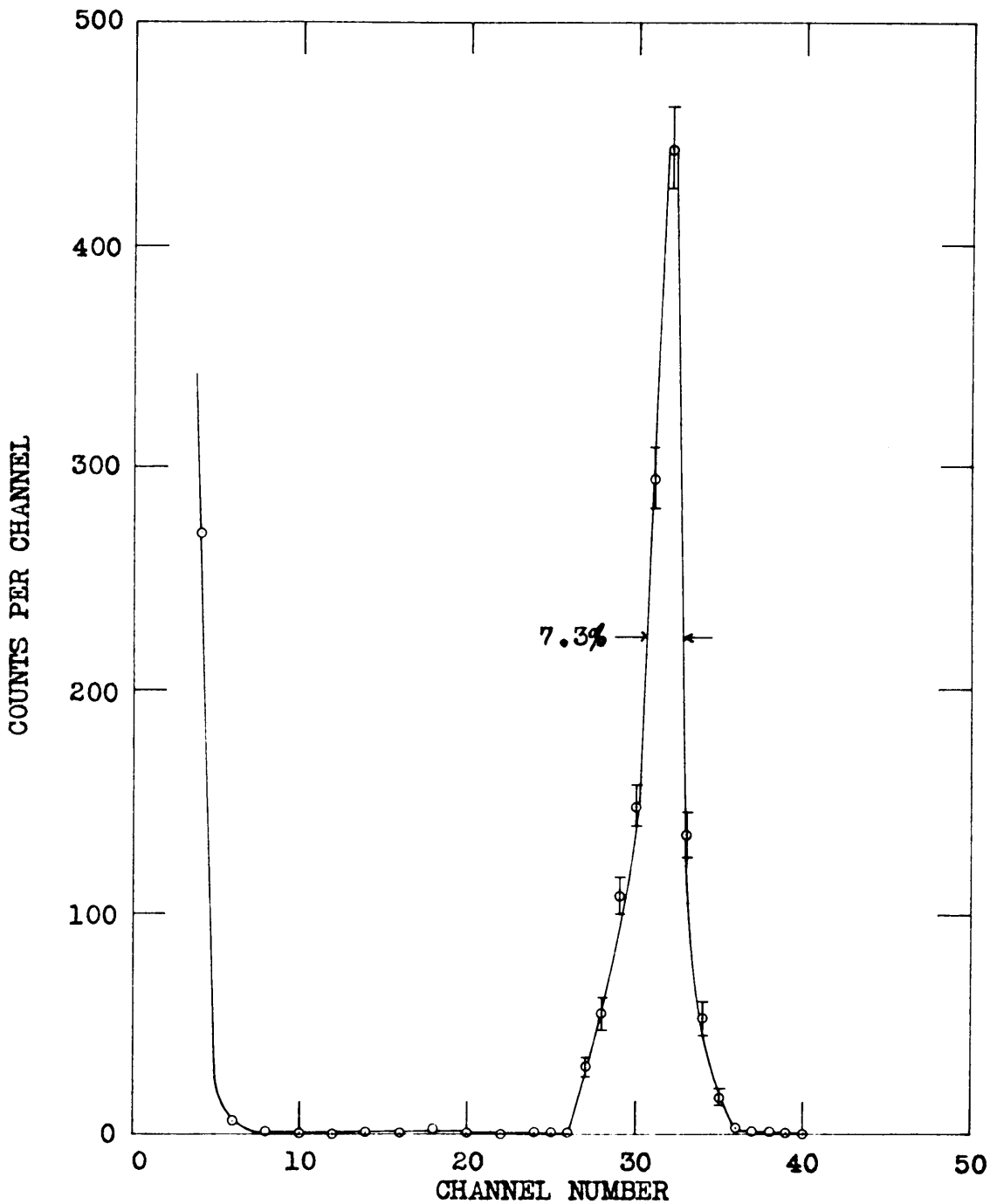


Figure 15. Pulse-height spectrum of neutrons obtained with the proton recoil telescope.



and paraffin mixture located directly over the sensitive area of the detector. With the detector and preamplifier as one unit, a traverse of the thermal column in the reactor was taken. The integral response of the detector above a given bias setting for the traverses both in and out for the muvistor preamplifier are shown in figure 16. The resultant slopes for the respective traverses are  $0.0363 \pm .0022 \text{ cm}^{-1}$  and  $0.0358 \pm .0018 \text{ cm}^{-1}$ . The pulse-height spectrum of the same traverses for the transistor preamplifier are shown in figure 17. The resultant slopes are  $0.0351 \pm .0020 \text{ cm}^{-1}$  and  $0.0350 \pm .0018 \text{ cm}^{-1}$  for the respective traverses. The discrepancy of the traverses in and out are within experimental error. The slight difference in the slopes obtained with the two preamplifiers may be accounted for by the fact that the muvistor preamplifier was much bigger and could have disturbed the flux more than the smaller transistor preamplifier.

To show the possible use of the surface-barrier detector as an alpha spectrometer, one spectrum was taken of an alpha source, which is a mixture of several nuclides, that is presently used in the modern physics laboratory. This spectrum shows alpha particles ranging from low energies up to approximately nine mev. This spectrum is shown in figure 18.

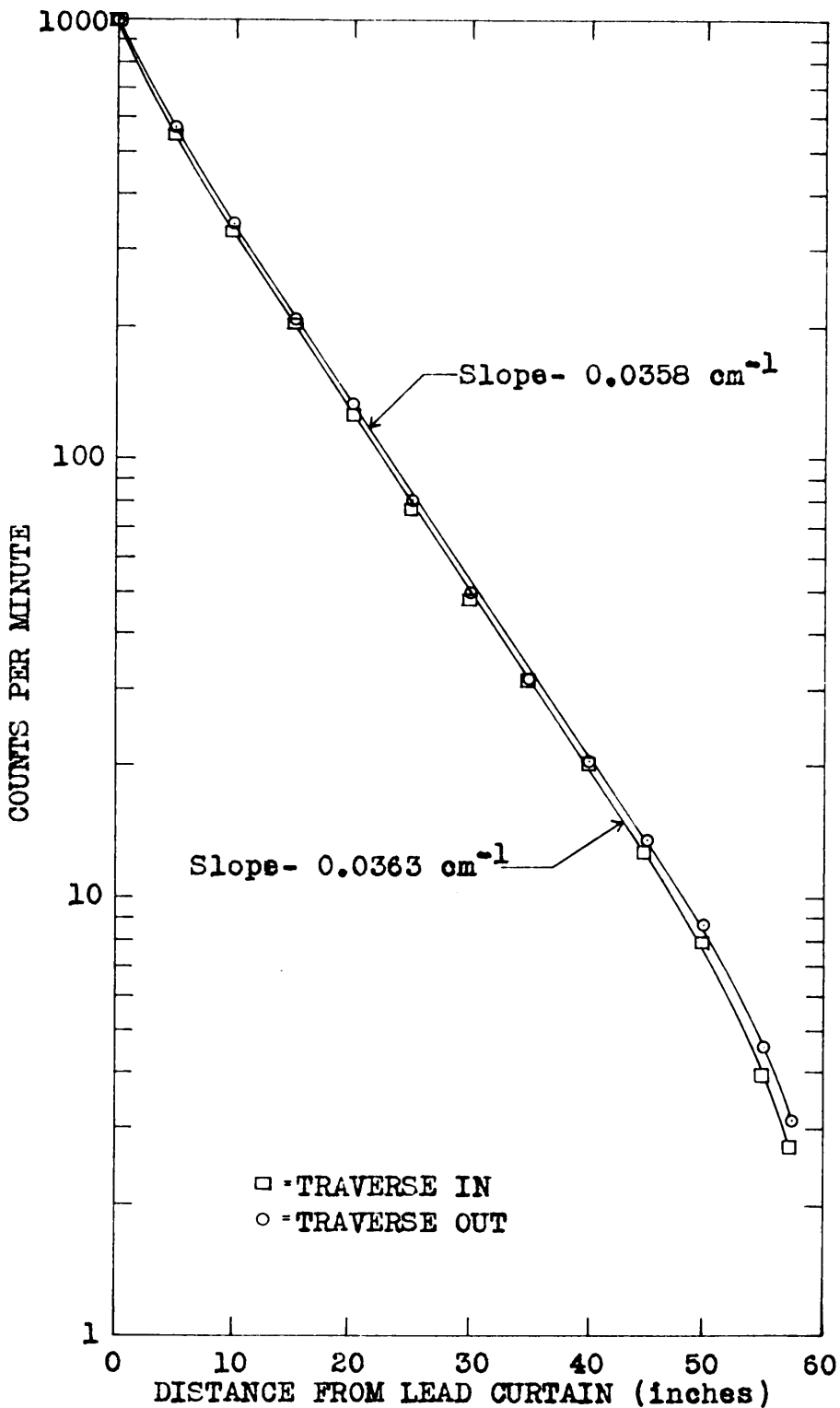


Figure 16. Resultant curves for traverse of thermal column with nuvistor preamplifier.

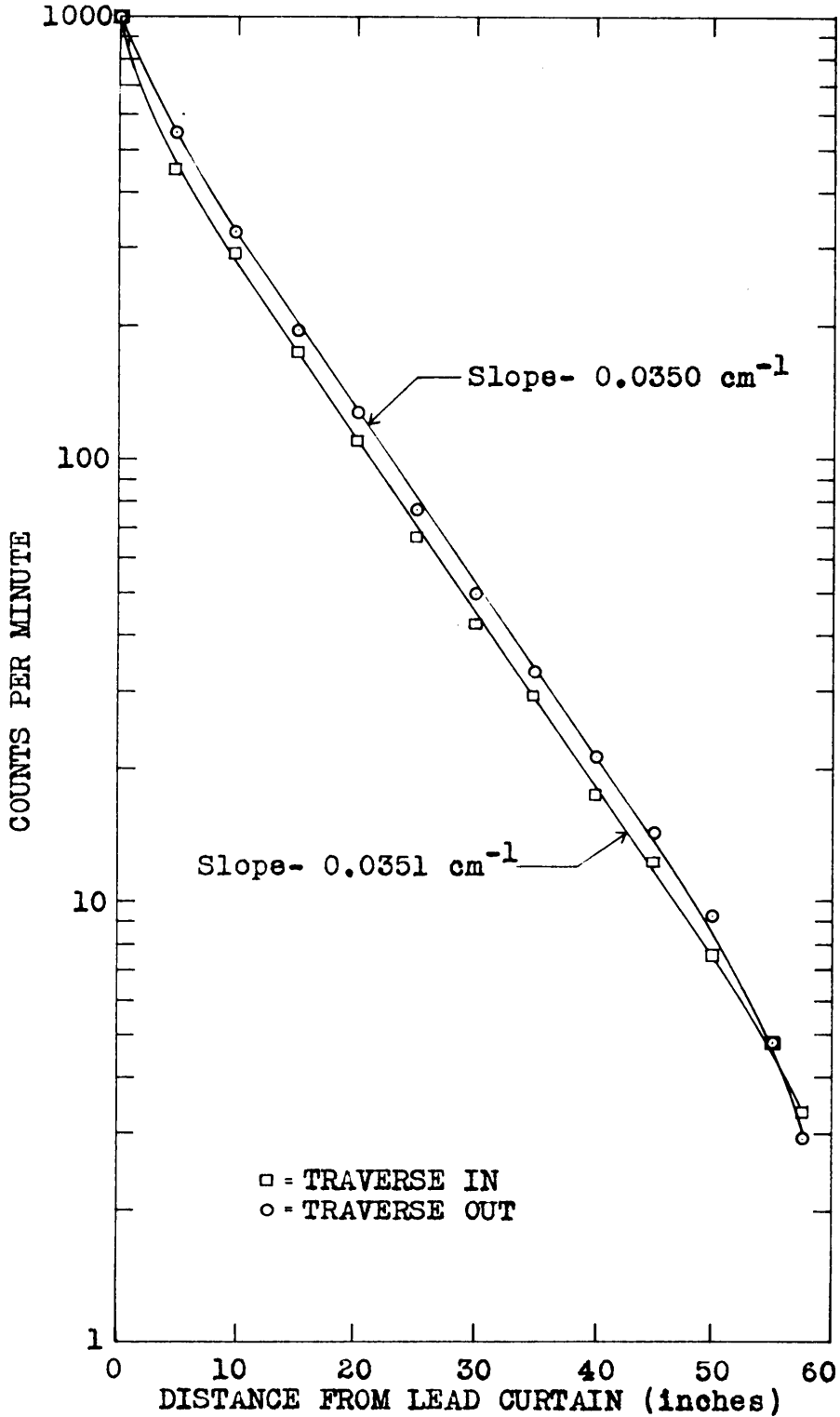


Figure 17. Resultant curves for traverse of thermal column with transistor preamplifier.

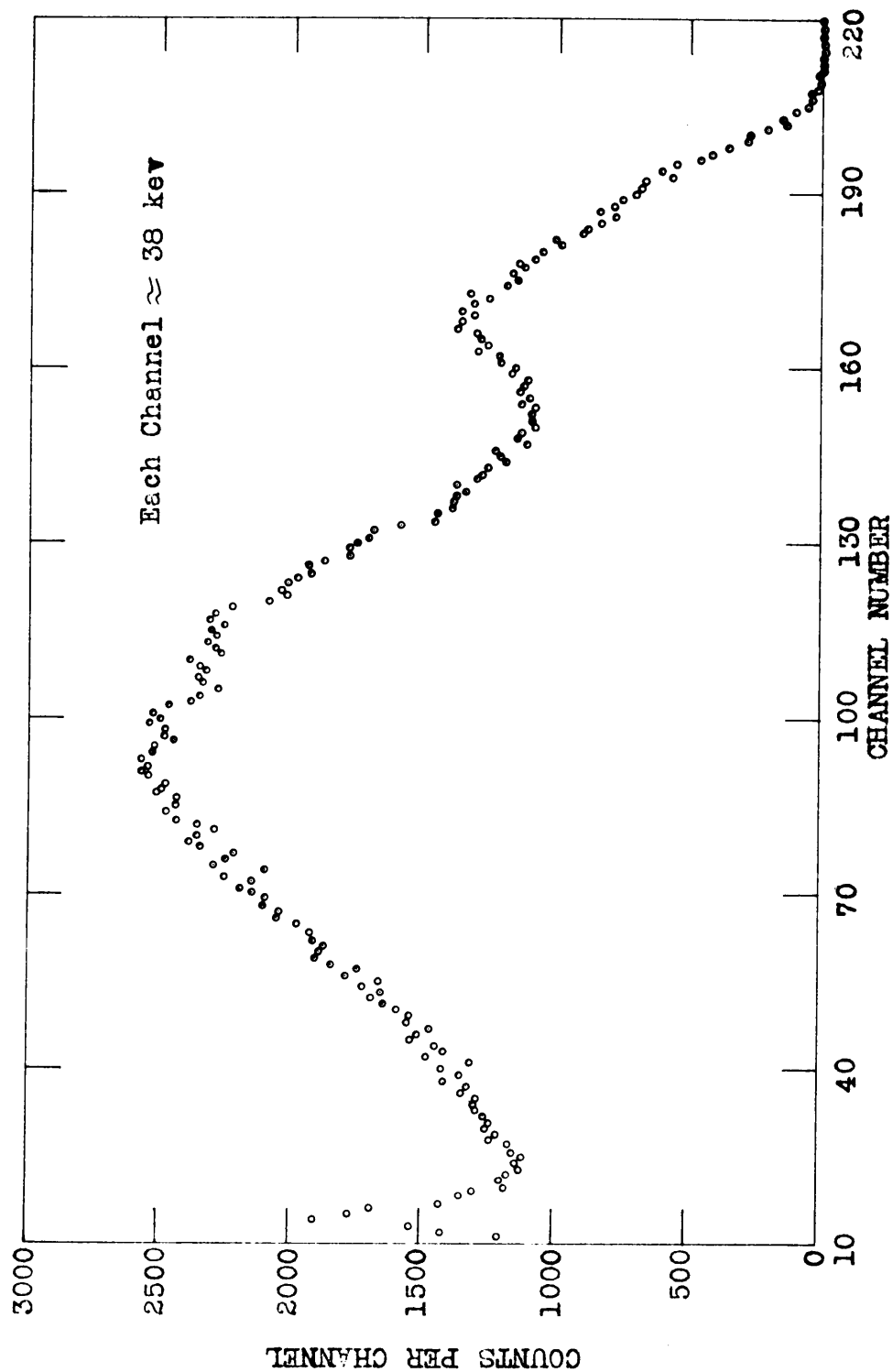


Figure 18. Pulse-height spectrum of modern physics laboratory alpha source.

### VIII. INTERPRETATION OF EXPERIMENTAL DATA

The experimental results observed in performing this research compare favorably with the results published by other experimenters. The results obtained in making the pulser characteristic checks on the electronic equipment agree with the results on similar equipment published by Halbert and Blankenship (13). The resolutions obtained by them were 0.5-0.7 per cent. The resolutions obtained in this work were 0.59 per cent and 0.48 per cent for the muvistor and transistor preamplifiers respectively. However, the results obtained in the alpha particle check did not agree quite as well as expected from the results of the pulser tests. The resolutions obtained with the monoenergetic alpha source were 3.8 per cent and 7.0 per cent for the muvistor and transistor preamplifiers respectively. These are considerably higher than the values furnished with the detectors by the manufacturer (29). The manufacturer obtained a resolution of 0.37 per cent at a pressure of 0.02 mm Hg using the CRTEC Model 101 preamplifier and Model 201 amplifier. The electronics used in this research work are comparable with their electronics. One reason for the difference could lie in the source. The source used in this research was a deposit of  $Po^{210}$  on a silver foil. One effect, as previously discussed, that could have caused poor resolution is the straggling effect produced by contamination of the source with surface grease and dust. This effect would increase the energy spread of the alpha particles and decrease the resolution. This

was observed in performing this research. The initial source was contaminated with grease and dust producing a large increase in the energy spread so a second source was prepared. One other effect that could cause poor resolution is the spreading of the energies of the alpha particles passing through a thin layer of polonium, which has a large  $-dE/dx$  for alpha particles. The energy spreads that could be caused by these effects are the same order of magnitude as the poor resolution obtained.

The experimental data shown in figures 16 and 17 which were obtained in performing the traverses in the thermal column of the reactor indicate that the detector and preamplifier as an unit make a satisfactory thermal neutron detector. The slopes obtained from the straight portions of the experimental curves compare very favorably with slopes obtained previously by Stam (34). He obtained his data by activation of gold foils and also by using a fission chamber. Using the fission chamber Stam (34) traversed the thermal column with the reactor running at a power of 0.6 watts. The counting rate at the lead curtain was 71,000 counts per minute. Since the efficiency of the surface-barrier detector is less than that of the fission chamber, it was necessary to run the reactor at a power of 5 watts to obtain a counting rate of 55,000 counts per minute at the lead curtain. The average slope from several traverses in this experiment was  $0.0356 \text{ cm}^{-1}$  which agrees within experimental error with the value of  $0.0360 \text{ cm}^{-1}$  obtained previously (34).

The last and most important phase of the experiment was the testing of the proton recoil telescope in order to investigate the feasibility of constructing a neutron spectrometer. The results obtained here were much better than expected on the bases of the crudeness of this first model of the spectrometer, although, as previously mentioned, the calculated resolution agreed well with the experimental data. Using the proton recoil telescope as a fast neutron detector the neutron pulse-height spectrum of the d-d reaction from the Cockroft-Walton accelerator at a back angle of  $176^\circ$  was taken. The neutron energy at this angle was about 2.1 mev. The average resolution of the original and confirming run was 7.9 per cent. This is much lower than data reported by Cochran and Henry (7), Johnson and Trial (17), and Perlow (30). Their data indicate resolutions on the order of 15 to 20 per cent. Some of this could be accounted for in the collimation and type of detectors used. They performed their work using proportional counters which are rather sensitive to background radiation and their telescopes had large solid angles. The surface-barrier detectors used in the present work are better in both of these respects. They are very insensitive to background radiation, and their compact size allows the solid angle to be made small. In addition, the present detectors have an inherently good energy resolution.

## IX. SUMMARY

The objects of this research were to construct the necessary equipment for use with the solid state surface-barrier detectors employed as neutron detectors. This research also had the ultimate aim of showing the possibility of producing a neutron spectrometer using the proton recoil telescope with the surface-barrier detector. These objects were fulfilled.

From the results with the proton recoil telescope, there is a possibility of producing a neutron spectrometer using the proton recoil telescope and surface-barrier detectors. However, if a thinner radiator were employed, the energy spread of the recoiling protons would be less and ultimately improve the resolution. The radiator in this trial had a large  $-dE/dx$  for protons and caused considerable straggling in the proton energy. Besides the straggling produced by the radiator there was some effect on energy spread by the collimator. A collimator with essentially an infinite number of baffles was used, since it consisted of a hole drilled through the collimator material. If the number of baffles were decreased, the possibility of protons being scattered from the collimator walls and being detected, but at a lower energy, would be eliminated. With this better collimation there will be a smaller solid angle and ultimately better resolution. Evacuating the chamber should also



improve the resolution. Thus with some improvements, the present equipment could be changed into a neutron spectrometer with good energy resolution.

## X. ACKNOWLEDGMENTS

The author wishes to express his appreciation to his advisor, Professor A. Keith Furr, for his aid and advice during the project. The author also wishes to thank Dr. J. Stoltzfus for his advice, Dr. McPherson for the preparation of the alpha sources, Professor J. Ryan for the use of his equipment, and fellow students for running the Cockcroft-Walton accelerator and reactor while obtaining the neutron spectrum data.

## XI. BIBLIOGRAPHY

1. Bame, Haddad, Perry, Smith, and Swartz, Review of Scientific Instruments, Vol. 31, 911 (1960).
2. Bell, R. E., Annual Review of Nuclear Science, Vol. 4, 93 (1954).
3. Blankenship and Borkowski, Bulletin of American Physical Society, Series II, Vol. 5, 38 (1960).
4. Blankenship and Borkowski, IRE Transactions on Nuclear Science, Vol. NS-8, No. 1, 17 (1960).
5. Brooks, Annual Review of Nuclear Science, Vol. 6, 215 (1956).
6. Brown, IRE Transactions on Nuclear Science, Vol. NS-8, No. 1, 2 (1960).
7. Cochran and Herry, Review of Scientific Instruments, Vol. 26, 757 (1955).
8. Fairstein, Review of Scientific Instruments, Vol. 27, 475 (1956).
9. Friedland, et al., Nucleonics, Vol. 18, No. 2, 54 (1960).
10. Fowler and Brolley, Jr., Reviews of Modern Physics, Vol. 28, 103 (1956).
11. Gossick, Review of Scientific Instruments, Vol. 26, 754 (1955).
12. Greiner, Semiconductors Devices and Applications, McGraw-Hill Book Company, New York, 1961.
13. Halbert and Blankenship, Nuclear Instruments and Methods, Vol. 8, No. 1, 106 (1960).
14. Halbert, Blankenship and Goldman, Bulletin of American Physical Society, Series II, Vol. 5, 38 (1960).
15. Harvey, Annual Review of Nuclear Science, Vol. 10, 235 (1960).
16. Hill, Physical Review, Vol. 87, 1034 (1952).
17. Johnson and Trial, Review of Scientific Instruments, Vol. 27, No. 7, 468 (1956).

18. Kendall, Annual Review of Nuclear Science, Vol. 9, 343 (1959).
19. Kingston, (ed.), Semiconductor Surface Physics, University of Pennsylvania Press, Philadelphia, Pennsylvania, (1957).
20. Love and Murray, ORNL Central Files No. 60-5-121.
21. Mann and Managan, Review of Scientific Instruments, Vol. 31, No. 8, 908 (1960).
22. Manov, Annual Review of Nuclear Science, Vol. 4, 51 (1954).
23. Marion and Fowler, Fast Neutron Physics, Part I, Interscience Publishers, Inc., New York, 1960.
24. Mayer and Gossick, Review of Scientific Instruments, Vol. 27, 407 (1956).
25. McKay, Physical Review, Vol. 84, 829 (1951).
26. McKay and McAfee, Physical Review, Vol. 91, 1079 (1953).
27. McKenzie and Bromley, Bulletin of American Physical Society, Series II, Vol. 4, 457 (1959).
28. Nordburg, Bulletin of American Physical Society, Series II, Vol. 4, 457 (1959).
29. Oak Ridge Technical Enterprises Corporation, Silicon Radiation Detectors, (1961).
30. Perlow, Review of Scientific Instruments, Vol. 27, No. 7, 460 (1956).
31. Rossi and Staub, Ionization Chambers and Counters, McGraw-Hill Book Company, New York (1949).
32. Semiconductor Detectors, Nucleonics, Vol. 18, No. 5, 98 (1960).
33. Shive, The Properties, Physics and Design of Semiconductor Devices, D. Van Nostrand Company, New York, 1959.
34. Stam, Performance and Characteristics of the V.P.I. Training and Research Reactor, M.S. Thesis, Virginia Polytechnic Institute (September, 1961).

35. Walter, Dabbs, and Roberts, Bulletin of American Physical Society, Series II, Vol. 3, 304 (1958).
36. Walter, Dabbs and Roberts, Bulletin of American Physical Society, Series II, Vol. 3, 181 (1958).
37. Walter, Dabbs, and Roberts, Bulletin of American Physical Society, Series II, Vol. 5, 38 (1960).
38. Warschauer, Semiconductors and Transistors, McGraw-Hill Book Company, New York, 1959.
39. Watt, Physical Review, Vol. 87, 1037 (1952).

**The vita has been removed from  
the scanned document**

## ABSTRACT

In this research an investigation of the use of silicon surface-barrier detectors for neutron detection was carried out. Several pieces of equipment, such as charge sensitive low noise preamplifiers and bias supplies needed to perform this investigation, were constructed. The preamplifiers were constructed in probe form so that neutron flux distribution measurements could be made. The neutron interacts with a mixture of  $B^{10}$  and paraffin, and the alpha particle from the  $B^{10}(n, \alpha)Li^7$  reaction is detected with a silicon surface-barrier detector. The feasibility of producing a neutron spectrometer employing a proton recoil telescope was investigated, since the energy of the incoming neutron can be derived from the energy of the recoiling proton. It was shown that it should be possible to construct a neutron spectrometer with good energy resolution using the proton recoil technique.